



Article

# Dental Pulp Inflammation Initiates the Occurrence of Mast Cells Expressing the $\alpha_1$ and $\beta_1$ Subunits of Soluble Guanylyl Cyclase

Yüksel Korkmaz <sup>1,\*</sup> , Markus Plomann <sup>2</sup>, Behrus Puladi <sup>3</sup>, Aysegül Demirbas <sup>4,5</sup>, Wilhelm Bloch <sup>6</sup> and James Deschner <sup>1</sup>

- <sup>1</sup> Department of Periodontology and Operative Dentistry, University Medical Center, Johannes Gutenberg University Mainz, 55131 Mainz, Germany
- <sup>2</sup> Center for Biochemistry, Faculty of Medicine, University of Cologne, 50931 Cologne, Germany
- <sup>3</sup> Department of Oral and Maxillofacial Surgery, University Hospital RWTH Aachen, RWTH Aachen University, 52074 Aachen, Germany
- <sup>4</sup> Department of Restorative Dentistry, Faculty of Dentistry, Mugla Sıtkı Kocman University, Mugla 48000, Turkey
- <sup>5</sup> Department of Restorative Dentistry, Faculty of Dentistry, Ege University, Izmir 35040, Turkey
- <sup>6</sup> Department of Molecular and Cellular Sport Medicine, German Sport University Cologne, 50933 Cologne, Germany
- \* Correspondence: yueksel.korkmaz@unimedizin-mainz.de

**Abstract:** The binding of nitric oxide (NO) to heme in the  $\beta_1$  subunit of soluble guanylyl cyclase (sGC) activates both the heterodimeric  $\alpha_1\beta_1$  and  $\alpha_2\beta_1$  isoforms of the enzyme, leading to the increased production of cGMP from GTP. In cultured human mast cells, exogenous NO is able to inhibit mast cell degranulation via NO-cGMP signaling. However, under inflammatory oxidative or nitrosative stress, sGC becomes insensitive to NO. The occurrence of mast cells in healthy and inflamed human tissues and the in vivo expression of the  $\alpha_1$  and  $\beta_1$  subunits of sGC in human mast cells during inflammation remain largely unresolved and were investigated here. Using peroxidase and double immunohistochemical incubations, no mast cells were found in healthy dental pulp, whereas the inflammation of dental pulp initiated the occurrence of several mast cells expressing the  $\alpha_1$  and  $\beta_1$  subunits of sGC. Since inflammation-induced oxidative and nitrosative stress oxidizes  $\text{Fe}^{2+}$  to  $\text{Fe}^{3+}$  in the  $\beta_1$  subunit of sGC, leading to the desensitization of sGC to NO, we hypothesize that the NO- and heme-independent pharmacological activation of sGC in mast cells may be considered as a regulatory strategy for mast cell functions in inflamed human dental pulp.

**Keywords:** inflammation; dental pulp; pulpitis; mast cells; nitric oxide; soluble guanylyl cyclase; cGMP; ROS; peroxynitrite; RNS



**Citation:** Korkmaz, Y.; Plomann, M.; Puladi, B.; Demirbas, A.; Bloch, W.; Deschner, J. Dental Pulp Inflammation Initiates the Occurrence of Mast Cells Expressing the  $\alpha_1$  and  $\beta_1$  Subunits of Soluble Guanylyl Cyclase. *Int. J. Mol. Sci.* **2023**, *24*, 901. <https://doi.org/10.3390/ijms24020901>

Academic Editors: Thimios A. Mitsiadis, Christian Morsczeck and Takayoshi Yamaza

Received: 7 November 2022

Revised: 6 December 2022

Accepted: 27 December 2022

Published: 4 January 2023



**Copyright:** © 2023 by the authors. Licensee MDPI, Basel, Switzerland. This article is an open access article distributed under the terms and conditions of the Creative Commons Attribution (CC BY) license (<https://creativecommons.org/licenses/by/4.0/>).

## 1. Introduction

The inter- and intracellular molecule nitric oxide (NO)-sensitive soluble guanylyl cyclase (sGC) is a heterodimeric enzyme with an  $\alpha$  and  $\beta$  subunit [1,2]. The redox state of the heme moiety of the  $\beta_1$  subunit of sGC is critical for the NO-heme iron interaction within the  $\beta_1$  subunit in order to activate sGC heterodimers [3,4]. Heme iron in the reduced state ( $\text{Fe}^{2+}$ ) is required for the binding of NO to the  $\beta_1$  subunit of sGC, whereas heme iron in the oxidized state ( $\text{Fe}^{3+}$ ) causes the enzyme to be insensitive to NO and decreases cGMP production [3–6]. Under physiological conditions, NO binds to heme in the  $\beta_1$  subunit of sGC and activates the enzyme containing reduced  $\text{Fe}^{2+}$  in the  $\alpha_1\beta_1$  and  $\alpha_2\beta_1$  isoforms. In the heterodimeric  $\alpha_1\beta_1$  and  $\alpha_2\beta_1$  isoforms, sGC induces the production of cGMP, resulting in cell-specific functions such as vasodilation [3,7], the inhibition of vascular smooth muscle proliferation [8,9], leukocyte recruitment and platelet aggregation [9,10], and the modulation of neurotransmission [11,12].

Mast cells originate from the yolk sac during embryogenesis and after birth from CD34+ hematopoietic stem cells in the bone marrow via definitive hematopoiesis [13,14]. Immature mast cells enter the tissues and undergo their final maturation into connective tissue mast cells or mucosal mast cells after receiving an appropriate signal from the tissue environment [14,15]. Mast cells are activated by bacteria and their products via innate immunity through pattern recognition receptors, such as TLRs and NOD-like receptors, expressed in mast cells [16,17] and promote adaptive immunity by modulating dendritic cell migration and immunological cellular processes in lymph nodes [17–19]. In adaptive immunity, mast cells are sensitized by different classes of immunoglobulins via Fc receptors (FcRs) [19,20]. Mast cells are activated when IgE bound to FcεRI receptors is crosslinked by bi- or multivalent antigens [21,22]. Upon activation by their receptors, mast cells release histamine, tryptase, and chymase from their secretory granules via degranulation [21,23]. Mast cells produce lipid mediators (prostaglandins and leukotrienes) as well as proinflammatory and chemotactic cytokines (tumor necrosis factor (TNF), interleukin (IL)-6, IL-4, IL-5, IL-1β, IL-10, IL-13, CCL1, CCL2, CXCL1, and CXCL8) [21,23]. The mediators secreted by mast cells contribute to host immunity and inflammation associated with various diseases [20,23,24].

NO is produced in mast cells through the activity of eNOS, nNOS, and iNOS [25–27]. In cultured mast cells, NO is able to inhibit mast cell degranulation [28,29] via the NO–cGMP signaling cascade [30]. NO donors inhibit histamine release and mast cell degranulation, whereas NO inhibitors enhance LPS-induced histamine release in mast cells [28]. The role of sGC in mast cells was investigated in cultured mast cells using the inhibitor 1H-[1,2,4]oxadiazolo [4,3-a]quinoxalin-1-one (ODQ), specific for sGC [30]. In cultured human mast cells, it was found that NO donors were able to increase the formation of cGMP through the release of exogenous NO [30]. However, the inflammation-dependent formation of superoxide ( $O_2^-$ ) and peroxynitrite ( $ONOO^-$ ) oxidizes sGC, leading to the insensitivity of sGC to NO [3,5]. Therefore, under inflammatory conditions, sGC may only be activated in an NO- and heme-independent manner. Since the pharmacological NO- and heme-independent activation or stimulation of sGC requires the presence of the enzyme at the protein level [31–34], it is necessary to clarify whether sGC occurs at the protein level in mast cells in tissues under physiological and inflammatory conditions.

Inflammation in the dental pulp occurs as a consequence of bacterial infection caused by dentin caries [35–38]. The carious bacteria and their products reach the dental pulp through the dentinal tubules, initiating an immunological host defense reaction in the dental pulp [39,40]. Host defenses in the dental pulp are regulated by the innate and adaptive immune responses [40–43], and mast cells are involved in their regulation upon bacterial infection [17,18,24,44–46]. The presence of mast cells in healthy [47] and inflamed [48] dental pulp has been described previously. However, the occurrence and the role of mast cells in healthy dental pulp and in pulp necrosis as well as chronic and acute pulp inflammation remain to be elucidated. Therefore, in the present study, we addressed the presence of mast cells and the  $\alpha_1$  and  $\beta_1$  subunits of sGC in these cells in healthy and inflamed dental pulp.

## 2. Results

In cells from healthy dental pulp (Figure 1A–D), MCT was not found (Figure 1E–H). In cells from inflamed dental pulp (Figure 2A–D), MCT (Figure 2E–H) was detected in several mast cells. In the inflamed dental pulp, the  $\alpha_1$  (Figure 3A–P) and  $\beta_1$  (Figure 4A–P) subunits of sGC were colocalized with MCT in mast cells at different staining intensities (Figure 5).

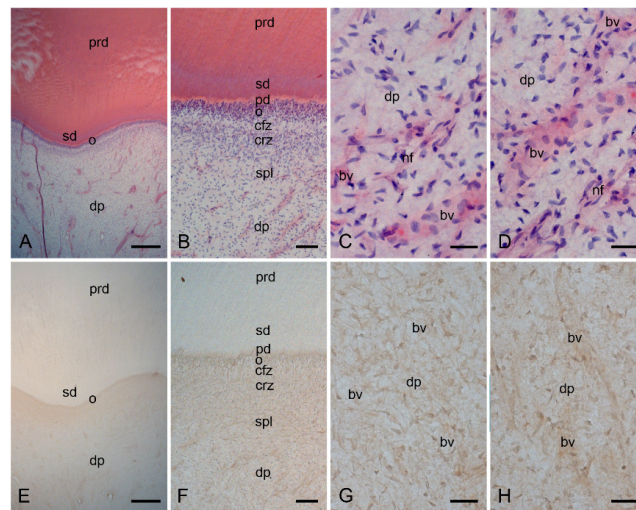


**Figure 1.** Histopathological characterization of healthy human dentin–pulp complex via hematoxylin and eosin (HE) staining and the expression of mast cell tryptase (MCT) in cells from consecutive sections of healthy human dental pulp. The structural order of the healthy dentin–pulp complex in the overview image (A) is visible in the detailed images as primary dentin (prd), secondary dentin (srd), predentin (pd), odontoblast layer (o), cell-free zone (cfz), and cell-rich zone (crz) (B), and blood vessels (bv), nerve fibers, and numerous pulp cells in the human dental pulp (dp) (C,D). In the cells of the healthy dental pulp of the consecutive section, the immunohistochemical localization for MCT is not visible in the overview (E) and detailed images (F–H). Scale bars: (A,E) = 500  $\mu$ m; (B,F) = 100  $\mu$ m; (C,D,G,H) = 30  $\mu$ m.

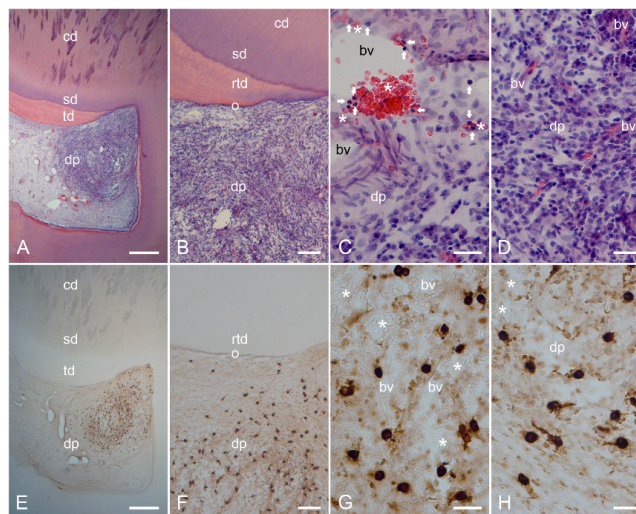


**Figure 2.** Histopathological characterization of inflamed human dentin–pulp complex by hematoxylin and eosin (HE) staining and the expression of mast cell tryptase (MCT) in cells from consecutive sections of inflamed human dental pulp. In deep dentin caries of the dentin–pulp complex, the carious dentin lesion sites (cd) with destroyed primary dentin, secondary dentin (srd), and the formation of reactive tertiary dentin (rtd) are visible (A). The structural and cellular order of the healthy dentin–pulp complex is not visible in the carious dentin–pulp complex (A,B). Beneath the carious lesion, there are severe chronic and acute inflammatory areas with numerous different inflammatory cells and dilated blood vessels (B–D). Neutrophilic granulocytes (arrows) associated with numerous erythrocytes (asterisks) are found in the lumen and wall of the blood vessels (C). In the consecutive section of the inflamed human dental pulp, MCT is detected in mast cells within chronically and acutely inflamed areas, which are seen in the overview (E) and detailed images (F–H). The mast cells are associated with blood vessels, which contain numerous erythrocytes (asterisks; G,H). Scale bars: (A,E) = 500  $\mu$ m; (B,F) = 100  $\mu$ m; (C,D,G,H) = 30  $\mu$ m.

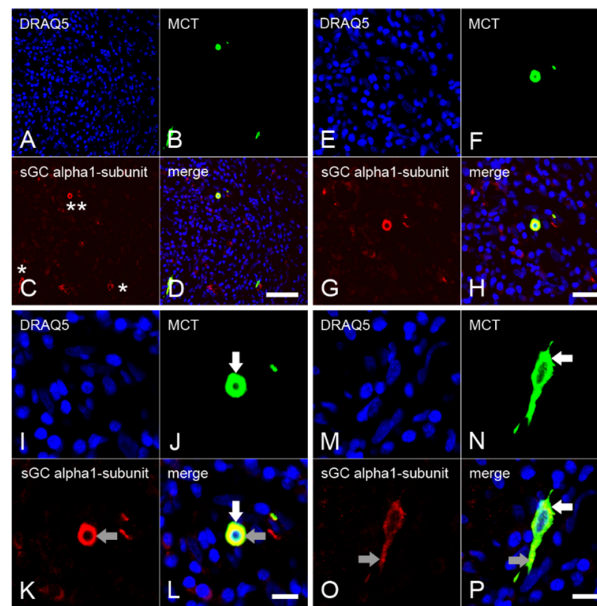


**Figure 3.** Colocalization of the  $\alpha_1$  subunit of sGC with MCT in mast cells in chronically inflamed human dental pulp. Numerous inflammatory cells with DRAQ5 nuclear staining are visible in the overview images of chronically inflamed human dental pulp (A). MCT (B) is colocalized with the sGC  $\alpha_1$  subunit (C) in some inflammatory cells with strong ((C), two asterisks) and weak ((C), one asterisk) staining intensities (D). Detailed images show the cytoplasmic subcellular colocalization of MCT with the sGC  $\alpha_1$  subunit at strong (E–L) and weak (M–P) immunostaining intensities in mast cells. In mast cells, the localizations of MCT (J,L,N,P) are shown with white arrows, while grey arrows show the  $\alpha_1$  subunit of sGC (K,L,O,P). Scale bars: A–D = 50  $\mu\text{m}$ ; E–H = 20  $\mu\text{m}$ ; I–P = 10  $\mu\text{m}$ .

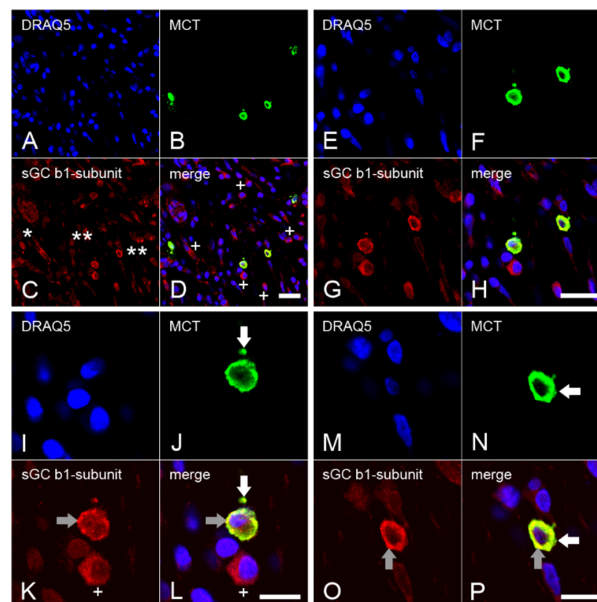


**Figure 4.** Colocalization of the  $\beta_1$  subunit of sGC with MCT in mast cells of chronically inflamed human dental pulp. Numerous inflammatory cells with DRAQ5 nuclear staining are present in the overview images of the chronically inflamed dental pulp (A). MCT (B) colocalizes with sGC  $\beta_1$  subunit (C) in a subpopulation of the inflammatory cells with strong ((C), two asterisks) and weak ((C), one asterisk) immunostaining intensities (D). In another subpopulation of cells that are MCT negative, the sGC  $\beta_1$  subunit is apparent (+ character in D,K,L). In the detailed images, the colocalization of MCT with the sGC  $\beta_1$  subunit in the cytoplasm of the mast cells is apparent (E–P). In mast cells, the localizations of MCT (J,L,N,P) are shown with white arrows, while the grey arrows show the  $\beta_1$  subunit of sGC (K,L,O,P). Scale bars: A–H = 20  $\mu\text{m}$ ; I–P = 10  $\mu\text{m}$ .

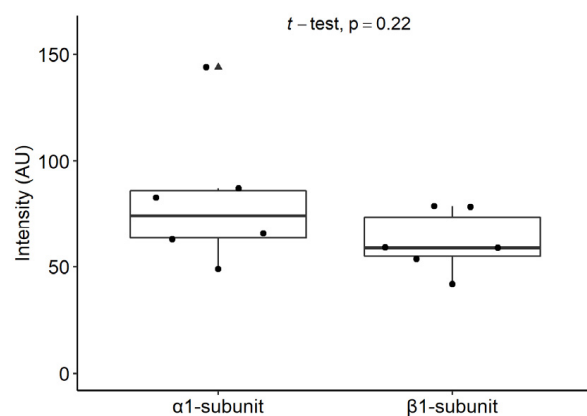


**Figure 5.** Staining intensities of the  $\alpha_1$  and  $\beta_1$  subunits of sGC in the mast cells of inflamed human dental pulp. Note that there was no significant difference between the staining intensities of the  $\alpha_1$  and  $\beta_1$  subunits of sGC in mast cells ( $p = 0.22$ ). Box and whisker plot shows maximum (upper vertical line), minimum (lower vertical line), median (horizontal line), and interquartile range (box). Dots are single measurements and triangles are outliers. A  $p$ -value  $< 0.05$  was considered as significant.

### 2.1. Characterization of the Healthy Human Dentin–Pulp Complex and the Expression of Mast Cell Tryptase (MCT) in Cells from Healthy Human Dental Pulp

In the healthy dentin–pulp complex, primary dentin, secondary dentin, and predentin were seen in a structural order (Figures 1A,B and S1A,B). The odontoblast layer, the cell-free and cell-rich layers, and the subodontoblastic plexus with nerve fibers and blood vessels were also identified in a cellular order in the healthy dentin–pulp complex (Figures 1A,B and S1A,B). The healthy dental pulp contained numerous cells (Figures 1C,D and S1C,D). Several pulpal stromal cells were identified around the blood vessels and nerve fibers (Figures 1C,D and S1C). Arterial and venous blood vessels of different sizes (arteries, veins, and capillaries) were accompanied by nerve fibers in the dental pulp (Figures 1B–D and S1C,D).

In cells of the healthy dental pulp, the immunohistochemical localization of MCT was not identified (Figure 1E–H).

### 2.2. Characterization of Inflamed Human Dentin–Pulp Complex and the Expression of Mast Cell Tryptase (MCT) in Cells from Inflamed Human Dental Pulp

The structural order found in the healthy dentin–pulp complex (Figures 1A–D and S1A–D) was not visible in the dentin–pulp complex inflamed by a carious lesion (Figures 2A–D and S1E–H). The deep dentin caries destroyed the primary and secondary dentin layers (Figures 2A and S1E). Beneath the carious lesion, tertiary dentin was found (Figures 2A,B and S1E,F). A strong lymphocytic infiltrate with numerous inflammatory cells was detected in the dental pulp underlying the carious region (Figures 2A,B and S1E,F). In the acute and subacute inflammatory areas, numerous neutrophilic granulocytes emerged from the dilated blood vessels (Figures 2C and S1G,H), whereas the blood vessels in the more lymphocytic inflammatory areas were destroyed and degraded (Figures 2D and S1H). In several cases, inflammation in the dental pulp occurred in mixed forms, e.g., chronic, subacute, and acute inflammation (Figures 2C,D and S1G,H).

Beneath the carious lesion in the dental pulp, some lymphocytic inflammatory areas were identified (Figures 2A,B and S2A,B). Necrotic changes, including destroyed blood vessels, were found in the center of some inflammatory areas (Figure S2B,D). Around these necrotically altered inflammation areas, severe acute and chronic inflammatory areas with numerous different inflammatory cells and destroyed blood vessels were observed (Figure S2B,C). In these acute and chronic inflammatory regions, mast cell tryptase (MCT) was detected in several mast cells showing a larger cytoplasmic area and larger nuclei with avidin-biotin-peroxidase staining (Figures 2E–H and S2E–H). The localization of MCT in mast cells was confirmed in chronically inflamed dental pulp by immunofluorescence staining (Figure S3A,B).

### 2.3. Expression of the $\alpha_1$ Subunit of sGC in Mast Cells from Inflamed Dental Pulp

The numerous inflammatory cells detected by nuclear staining with DRAQ5 showed severe inflammation in the dental pulp (Figure 3A,E,I,M). MCT was identified in a small subpopulation of inflammatory cells showing a larger cytoplasm and nucleus than the other inflammatory cells (Figure 3B,F,J,N). In some mast cells, the sGC  $\alpha_1$  subunit was detected with strong staining intensities (Figure 3C,G,K), while in other mast cells, the staining intensity was weak (Figures 3C and 4O). Upon colocalization, the sGC  $\alpha_1$  subunit was identified with subcellular MCT at both stronger (Figure 3I–L) and weaker (Figure 3M–P) staining intensities in the cytoplasm. In a very small subpopulation of immune cells, the sGC  $\alpha_1$  subunit was found in the cytoplasm without colocalization with MCT (Figure 3D,H,L).

### 2.4. Expression of the $\beta_1$ Subunit of sGC in Mast Cells from Inflamed Dental Pulp

The presence of numerous nuclei of inflammatory cells detectable by DRAQ5 indicated severe inflammation in the dental pulp (Figure 4A,E,I,M). MCT was detected in a small subpopulation of inflammatory cells showing a large cytoplasm and nuclei, whereas the other inflammatory cells contained small and round nuclei (Figure 4B,F,J,N). In some inflammatory cells, the sGC  $\beta_1$  subunit was identified with MCT at a weak staining intensity (Figure 4C), while a stronger intensity was detected in some other inflammatory cells (Figure 4C,G,K,O). In the double stainings, the sGC  $\beta_1$  subunit in mast cells colocalized with MCT in one subpopulation (Figure 4D,H,L,P), whereas no colocalization was observed in the other subpopulations of inflammatory cells (Figure 4D,H,L).

### 2.5. Immunohistochemical Controls

In control incubations of the avidin–biotin–peroxidase complex (Figure S5) and the immunofluorescence double staining methods (Figure S6), no immunohistochemical staining was found in cells from healthy and inflamed human dental pulps.

### 2.6. Quantification of the Data and Statistical Analysis

#### 2.6.1. Counting of Mast Cells in Healthy and Inflamed Dental Pulp

MCT was not detectable in any cells of the healthy human dental pulp ( $n = 6$ ). In the inflamed human dental pulp ( $n = 6$ ), MCT was detected in mast cells. When compared, the inflamed dental pulp showed different numbers of mast cells (cell counts  $111 \pm 16$  [mean  $\pm$  SEM]; 51–296 [range]), which can be explained by the different mixed inflammation states in the dental pulp.

#### 2.6.2. Staining Intensities of the $\alpha_1$ and $\beta_1$ Subunits of sGC in Mast Cells

The immunofluorescence staining intensities for the  $\alpha_1$  and  $\beta_1$  subunits of sGC showed similar results (Figure 5). No significant differences were found between the staining intensities of the  $\alpha_1$  and  $\beta_1$  subunits of sGC in mast cells from the inflamed human dental pulp ( $p = 0.22$ ).

## 3. Discussion

Histopathological studies of mast cells in inflamed tissues are required to elucidate their pathophysiological role in organ-specific inflammation [24]. Although NO production has been shown in mast cells [25,27], it is unclear whether NO-sensitive sGC occurs as an active heterodimer isoform in these cells under physiological and inflammatory conditions. In our study, we found that mast cells were not present in healthy dental pulps and only appeared in inflamed dental pulps. In severely inflamed dental pulps, we detected the expression of both the  $\alpha_1$  and  $\beta$  subunits of sGC in mast cells, indicating the existence of the  $\alpha_1\beta_1$  heterodimers of sGC at the protein level in mast cells during inflammation. In inflammation,  $O_2^-$  and  $ONOO^-$  oxidize sGC ( $Fe^{2+}$  to  $Fe^{3+}$  in the  $\beta_1$  subunit of sGC), leading to the insensitivity of sGC to NO [3–6]. Because  $O_2^-$  and  $ONOO^-$  have been detected at higher concentrations in inflamed dental pulp [49,50], we suggested that sGC might be

present as an  $\alpha_1\beta_1$  isoform in mast cells at the protein level and could be insensitive to NO in the oxidized state in these cells during the inflammation of human dental pulp.

In the present study, the inflammatory regions in human dental pulp showed the histopathological features of mixed inflammation, ranging from a necrotic region to regions with chronic, subacute, and acute inflammatory features. In necrotically altered inflammatory regions, where blood vessels were degraded, no mast cells were found. In inflamed dental pulps, mast cells were observed around blood vessels in chronic, subacute, and/or acute inflammatory regions. In chronically inflamed regions, numerous neutrophil granulocytes left the blood vessel walls and formed acute inflammatory areas in the pulp (Figures 2C and S1G,H). Due to their role as the first effector cells recruited to sites of inflammation, neutrophils are crucial cells in the regulation of acute immune responses during inflammation [51–54]. In inflammation, mast cells orchestrate immunity against pathogens by secreting cytokines that trigger neutrophil granulocyte recruitment [19,55–58]. Our results showed that mast cells in inflamed dental pulps strongly expressed the protease mast cell tryptase. Mast cell tryptase has been shown to be involved in neutrophil granulocyte recruitment during inflammation [59,60]. Therefore, it is reasonable to assume that neutrophil granulocyte recruitment during dental pulp inflammation may be regulated in part by mast cell tryptase.

The mechanism controlling the inflammatory response [61] in dental pulp is not well understood. Inflammation triggers the complex processes of innate and adaptive immunity that serve to resolve inflammation in the acute phase [62,63]. Acute inflammation occurs over a few days or weeks and requires the presence of an external stimulus [63]. However, with prolonged or more intense infiltration by various immune cells, acute inflammation can progress to chronic inflammation [63,64]. Chronic inflammation may persist well beyond the presence of the external stimuli for months or years, mediated by various immune cells [63]. The impact of mast cell-derived inflammatory mediators on blood vessels may be a key driving force in the initiation, enhancement, or maintenance of acute and chronic inflammation [65]. In acute bacterial infections, the activity of mast cells leads to the early clearance of bacteria and resolution of inflammation [45,66]. In chronic inflammation, the modulation of inflammation by mast cells is much more complex, as interactions between mast cells and bacteria are prolonged [19,45]. Depending on the type of bacteria and the severity of infection, mast cells may promote rather than control chronic infections and can therefore exacerbate pathologic outcomes [45,66]. Mast cells secrete inflammatory mediators, accumulate, and proliferate in the inflammatory region, where they are long-lived [19,45]. In view of these findings and our results, we hypothesize that the treatment of a carious lesion during the acute inflammatory state of the dental pulp could improve its healing tendency through the functions of mast cells. If a carious lesion is not treated in time, the acute inflammation in the dental pulp may become chronic. In chronic pulp inflammation, mast cells promote inflammation by recruiting neutrophilic granulocytes, which may lead to the development of mixed (necrosis, chronic, subacute, and acute inflammatory regions) and thus uncontrolled inflammation.

We detected the  $\alpha_1$  and  $\beta_1$  subunits of sGC in the mast cells of inflamed dental pulp with different staining intensities. In some mast cells, the  $\alpha_1$  and  $\beta_1$  subunits of sGC were detected with a stronger staining intensity, whereas in other mast cells the intensity was lower. The difference in the intensities of the  $\alpha_1$  and  $\beta_1$  subunits of sGC suggests that mast cells exist in different functional states under inflammatory conditions and that the expression of the  $\alpha_1$  and  $\beta_1$  subunits of sGC depends on the chronic, subacute, or acute inflammation region-associated mast cell behavioral status.

In smooth muscle cells and in neurons, sGC is active as both  $\alpha_1\beta_1$  and  $\alpha_2\beta_1$  heterodimers. It is possible that sGC may also be activated as  $\alpha_2\beta_1$  heterodimers in subpopulations of mast cells negative for  $\alpha_1$  subunit of sGC. Therefore, future studies should clarify whether the  $\alpha_2$  subunit of sGC is present in mast cells at the protein level under in vivo conditions. We detected the  $\alpha_1$  subunit of sGC only in mast cells and in blood vessels, whereas the  $\beta_1$  subunit of sGC was detected in mast cells, blood vessels, and also in a

subpopulation of other inflammatory cells that were negative for MCT. Therefore, it should be clarified whether the  $\alpha_2$  subunit of sGC is also present in other immune cells that are negative for the  $\alpha_1$  subunit and MCT but positive for the  $\beta_1$  subunit.

In inflammation, the consumption of molecular oxygen ( $O_2$ ) by NADPH oxidase is increased in macrophages, neutrophil granulocytes, and dendritic cells that accumulate in the area of inflammation because NADPH oxidase transfers electrons from intracellular NADPH to  $O_2$  to generate superoxide ( $O_2^-$ ) [67]. The  $O_2^-$  generated by uncoupled endothelial nitric oxide synthase (eNOS) [68,69] or in macrophages, neutrophil granulocytes, and dendritic cells leads to the generation of the free radical hydrogen peroxide ( $H_2O_2$ ), which can lead to the formation of reactive oxygen species (ROS) and reactive nitrogen species (RNS) under inflammatory conditions [67,70]. The reduced  $Fe^{2+}$  state in the  $\beta_1$  subunit of sGC under physiological conditions and the oxidized  $Fe^{3+}$  state in the  $\beta_1$  subunit of sGC under inflammatory conditions are essential for determining the activity of sGC in a cell [3–6]. NO is produced in mast cells [25,27] and is able to inhibit mast cell degranulation and subsequent allergic inflammation [28,29]. NO donors inhibit histamine release and mast cell degranulation, whereas NO inhibitors enhance LPS-induced histamine release [28]. In cultured human mast cells, it has been shown that NO donors, such as DEA/NO, are able to increase the formation of cGMP through the release of exogenous NO [30], suggesting that cGMP may be formed via the activation of sGC by exogenous NO. However, during inflammation, sGC is oxidized (from  $Fe^{2+}$  to  $Fe^{3+}$ ) by higher concentrations of  $O_2^-$  and  $ONOO^-$ , leading to the insensitivity of sGC to NO [3–6]. Inflammation induces an increase in ROS and RNS concentrations [71,72]; this effect has been reported for inflamed dental pulp [49,50]. In addition, the inflammation-dependent synthesis of ROS and RNS in mast cells has also been described [70]. Based on these results, we suggest that higher ROS and RNS concentrations in mast cells under inflammatory conditions may oxidize the heme iron of sGC and desensitize it to NO. Thus, NO-dependent cGMP formation (cGMP may be formed also in part via particulate GC by natriuretic peptide) in mast cells under inflammatory conditions may be regulated by NO- and heme-independent sGC activators. Therefore, the use of sGC activators [31,33,34,73] and the modulation of sGC in mast cells may serve as a new treatment strategy for inflamed dental pulp.

Our results showed that mast cells were present in inflamed but not in healthy human dental pulp. In these mast cells, sGC was detectable at the protein level with both its  $\alpha_1$  and  $\beta_1$  subunits. Therefore, the NO- and heme-independent pharmacological activation of sGC in mast cells may be considered as a regulatory strategy for mast cell functions in inflamed human dental pulp. For example, indirect and direct pulp capping materials used in the treatment of deep dentin caries containing sGC activators could represent an immunomodulatory treatment option in the future.

#### 4. Materials and Methods

##### 4.1. Ethics Statement on the Collection of Human Molars

The Human Ethics Committee of the Heinrich-Heine University Düsseldorf approved the collection of human third molars extracted during orthodontic treatment (No. 2980).

##### 4.2. The Clinical Evaluation of Human Molars

The healthy molars were unrestored and clinically asymptomatic and showed no pain upon stimuli-induced testing and percussion. The carious molars showed clinically stimuli-induced, spontaneous, or percussion-induced pain and/or radiographic carious dentin and inflamed periodontal lesions.

##### 4.3. Tissue Preparation

The healthy ( $n = 6$ ) and inflamed third molars with deep dentin caries ( $n = 6$ ) were extracted from patients who had undergone orthodontic extraction treatment. The molars were immersion-fixed in a fixative containing 4% paraformaldehyde and 0.2% picric acid in 0.1 M phosphate-buffered saline (PBS), pH 7.4, for 48 h. The molars were demineralized in



4 M formic acid for 21 days. The non-carious and carious molars were cryoprotected with 30% sucrose solution in 0.1 M PBS, pH 7.4, for 48 h. The molars were frozen-embedded, stored at  $-82^{\circ}\text{C}$ , and frozen-sectioned on a cryostat at  $30\ \mu\text{m}$ .

#### 4.4. Histopathological Evaluation of Healthy and Inflamed Human Dental Pulp

Since the definitive diagnosis of pulpal inflammation is determined by histopathology, sections were stained with hematoxylin and eosin (HE) [49] and the results were characterized by histopathological diagnosis. In each subgroup of molars, immunohistochemical staining for mast cell tryptase (MCT), HLA-DR (monocytes, dendritic cells, and activated T and B cell markers), and CD68 (macrophage marker) were performed to characterize the leukocyte types in the healthy and inflamed human dentin-pulp complex and periodontium, as described previously [50,74].

#### 4.5. Specificity of sGC $\alpha_1$ Subunit and $\beta_1$ Subunit Antibodies

To detect the  $\alpha_1$  subunit of sGC in mast cells, we developed a specific polyclonal rabbit antibody against the human  $\alpha_1$  subunit of sGC (EP101278: ID0490; Eurogentec, Seraing, Belgium) that was characterized by immunohistochemistry and immunoblotting [75]. The specificity of the rabbit anti-human sGC  $\beta_1$  subunit antibody was verified with immunohistochemistry and immunoblotting using lung protein extracts from sGC $\beta_1^{+/+}$  and sGC $\beta_1^{-/-}$  mice [76].

#### 4.6. Immunohistochemical Methods

##### 4.6.1. Avidin-Biotin-Peroxidase Complex Method

Free-floating sections were incubated with 0.3%  $\text{H}_2\text{O}_2$  in 0.05 M Tris-buffered saline (TBS) for 20 min to inhibit endogenous peroxidase. Nonspecific immunoglobulin binding sites were blocked by the incubation of sections in blocking solution containing 5% normal goat serum (Vector, Burlingame, CA, USA) and 2% bovine serum albumin (BSA) (Sigma-Aldrich, Saint Louis, MO, USA). The sections of subgroups of healthy and carious molars were incubated with mouse monoclonal anti-human MCT (1:2000) (Santa Cruz Biotechnology, Santa Cruz, CA, USA), mouse monoclonal anti-human HLA-DR (1:2000) (eBioscience, San Diego, CA, USA), and mouse monoclonal anti-human CD68 (1:2000) (eBioscience). To detect the  $\alpha_1$  and  $\beta_1$  subunits in cells from the healthy and inflamed dental pulps, sections were incubated overnight with rabbit anti-human polyclonal sGC  $\alpha_1$  (1:1000) and  $\beta_1$  subunit (1:1000) antibodies at  $4^{\circ}\text{C}$ . Then, sections were incubated for 1 h with biotinylated goat anti-mouse IgG (1:1000) (Vector) or goat anti-rabbit IgG (1:500) (Vector). The sections were incubated for 1 h with avidin-biotin-peroxidase complex (1:100) (Vector). The immunohistochemical reaction was developed in all incubations for 15 min with 0.05% 3,3'-diaminobenzidine tetrahydrochloride (Sigma-Aldrich, St. Louis, MO, USA) in 0.05 M Tris-HCl buffer, pH 7.6, containing 0.01%  $\text{H}_2\text{O}_2$  and 0.01% nickel sulfate [49,50].

To control for secondary antibodies and avidin-biotin-peroxidase complex reagents (NGS, BSA, peroxidase complex), the omission of primary antibodies was performed as control staining.

##### 4.6.2. Immunofluorescence Double Staining Method

Free-floating sections were incubated with 5% normal goat serum and 2% BSA to block the nonspecific immunoglobulin binding sites of the secondary antibodies. The sections were incubated first with mouse anti-human MCT antibodies (Santa Cruz Biotechnology) at  $4^{\circ}\text{C}$ . Then, the sections were incubated with DyLight<sup>TM</sup> 488-conjugated goat anti-mouse IgG (Thermo Fischer Scientific, Waltham, MA, USA) for 1 h. In separate incubations, the sections were incubated with rabbit polyclonal anti-human  $\alpha_1$  subunit (1:1000) and rabbit polyclonal  $\beta_1$  subunit (1:1000) antibodies overnight at  $4^{\circ}\text{C}$ . Then, in separate incubations, the sections were incubated for 1 h with DyLight<sup>TM</sup> 550-conjugated goat anti-rabbit IgG (Thermo Fischer Scientific). To show the cell nuclei, sections were stained with DRAQ5 (Cell Signaling Technology, Frankfurt am Main, Germany) for 15 min. The sections were cover-

slipped with Aqua Poly/Mount (Polysciences Inc., Warrington, PA, USA) and analyzed with an LSM510 confocal microscope (Carl Zeiss, Jena, Germany) [49,74].

To control for the immunohistochemical reagents (NGS, BSA, secondary antibodies), sections were incubated in the absence of the first and secondary primary antibodies.

#### 4.7. Quantification of the Data and Statistical Analysis

##### 4.7.1. Counting of Mast Cells in the Inflamed Dental Pulp

In healthy ( $n = 6$  molars of 6 different patients) and inflamed ( $n = 6$  molars of 6 different patients) dental pulp, MCT-positive cells were visualized using conventional light microscopy. Sections stained with the avidin-biotin-peroxidase method were imaged at  $5\times$  magnification using an Olympus microscope (Olympus Deutschland GmbH, Hamburg, Germany) connected to the Cell F Imaging software (Olympus Soft Imaging Solutions GmbH, Münster, Germany). Then, an examiner (B.P.) counted the MCT-positive cells using the counting tool in QuPath (version 0.3.2) [77]. The source code for QuPath is available at <https://qupath.github.io>. The results were verified by a second examiner (Y.K.).

##### 4.7.2. Measurement of Immunofluorescence Staining Intensities

Three colour fluorescence images were taken with an LSM 510 META confocal microscope (Carl Zeiss, Oberkochen, Germany) and exported to QuPath (version 0.3.2) [77]. The cellular localizations of the  $\alpha_1$  subunit and  $\beta_1$  subunit of sGC in mast cells were annotated by one investigator (B.P.) and reviewed by a second investigator (Y.K.). The mean intensity of the red fluorescence (i.e., the staining intensities of the  $\alpha_1$  subunit and  $\beta_1$  subunit of sGC) was then exported to R.

##### 4.7.3. Statistical Analysis

Statistical analyses were performed in R (version 4.1.1). Data were tested for normal distribution using a Shapiro–Wilk test. Parametric values were tested for significant  $p$  values using an unpaired  $t$ -test. A  $p$  value  $< 0.05$  was considered significant. For cell counting, the mean and SEM (standard error of the mean) were calculated.

**Supplementary Materials:** The following supporting information can be downloaded at: <https://www.mdpi.com/article/10.3390/ijms24020901/s1>.

**Author Contributions:** Conceptualization, Y.K. and J.D.; methodology, Y.K., M.P., B.P., W.B. and J.D.; software, Y.K., B.P., W.B. and J.D.; validation, Y.K., M.P., B.P., W.B. and J.D.; formal analysis, Y.K., B.P., A.D. and W.B.; investigation, Y.K. and M.P.; resources, Y.K., M.P., A.D., W.B. and J.D.; data curation, Y.K., A.D., W.B. and J.D.; writing—original draft preparation, Y.K. and J.D.; writing—review and editing, Y.K., M.P., B.P., A.D., W.B. and J.D.; visualization, Y.K., M.P., B.P., W.B. and J.D.; supervision, Y.K., W.B. and J.D.; project administration, Y.K., M.P., W.B. and J.D.; funding acquisition, Y.K., M.P., A.D. and J.D. All authors have read and agreed to the published version of the manuscript.

**Funding:** This research received no external funding.

**Institutional Review Board Statement:** Approval for the study was obtained from the Human Ethics Committee of the Heinrich-Heine-University Düsseldorf, Germany (No. 2980, 28 January 2008).

**Informed Consent Statement:** Informed consent was obtained from all subjects involved in the study.

**Data Availability Statement:** Data sharing is not applicable to this article.

**Acknowledgments:** The authors would like to thank the patients who provided their teeth for this study. The authors would also like to thank Kurt Schneider for the English proofreading of the manuscript.

**Conflicts of Interest:** The authors declare no conflict of interest.

## References

1. Friebe, A.; Koesling, D. Regulation of nitric oxide-sensitive guanylyl cyclase. *Circ. Res.* **2003**, *93*, 96–105. [[CrossRef](#)] [[PubMed](#)]
2. Murad, F. Nitric oxide and cyclic guanosine monophosphate signaling in the eye. *Can. J. Ophthalmol.* **2008**, *43*, 291–294. [[CrossRef](#)] [[PubMed](#)]
3. Stasch, J.P.; Schmidt, P.M.; Nedvetsky, P.I.; Nedvetskaya, T.Y.; HS, A.K.; Meurer, S.; Deile, M.; Taye, A.; Knorr, A.; Lapp, H.; et al. Targeting the heme-oxidized nitric oxide receptor for selective vasodilatation of diseased blood vessels. *J. Clin. Investig.* **2006**, *116*, 2552–2561. [[CrossRef](#)] [[PubMed](#)]
4. Gladwin, M.T. Deconstructing endothelial dysfunction: Soluble guanylyl cyclase oxidation and the NO resistance syndrome. *J. Clin. Investig.* **2006**, *116*, 2330–2332. [[CrossRef](#)]
5. Rahaman, M.M.; Nguyen, A.T.; Miller, M.P.; Hahn, S.A.; Sparacino-Watkins, C.; Jobbagy, S.; Carew, N.T.; Cantu-Medellin, N.; Wood, K.C.; Baty, C.J.; et al. Cytochrome b5 Reductase 3 Modulates Soluble Guanylate Cyclase Redox State and cGMP Signaling. *Circ. Res.* **2017**, *121*, 137–148. [[CrossRef](#)]
6. Shah, R.C.; Sanker, S.; Wood, K.C.; Durgin, B.G.; Straub, A.C. Redox regulation of soluble guanylyl cyclase. *Nitric Oxide* **2018**, *76*, 97–104. [[CrossRef](#)]
7. Murad, F. Shattuck Lecture. Nitric oxide and cyclic GMP in cell signaling and drug development. *N. Engl. J. Med.* **2006**, *355*, 2003–2011. [[CrossRef](#)]
8. Münzel, T.; Feil, R.; Mülsch, A.; Lohmann, S.M.; Hofmann, F.; Walter, U. Physiology and pathophysiology of vascular signaling controlled by cyclic guanosine 3',5'-cyclic monophosphate-dependent protein kinase. *Circulation* **2003**, *108*, 2172–2183. [[CrossRef](#)]
9. Stasch, J.P.; Pacher, P.; Evgenov, O.V. Soluble guanylate cyclase as an emerging therapeutic target in cardiopulmonary disease. *Circulation* **2011**, *123*, 2263–2273. [[CrossRef](#)]
10. Ahluwalia, A.; Foster, P.; Scotland, R.S.; McLean, P.G.; Mathur, A.; Perretti, M.; Moncada, S.; Hobbs, A.J. Antiinflammatory activity of soluble guanylate cyclase: cGMP-dependent down-regulation of Pselectin expression and leukocyte recruitment. *Proc. Natl. Acad. Sci. USA* **2004**, *101*, 1386–1391. [[CrossRef](#)]
11. Friebe, A.; Koesling, D. The function of NO-sensitive guanylyl cyclase: What we can learn from genetic mouse models. *Nitric Oxide* **2009**, *21*, 149–156. [[CrossRef](#)] [[PubMed](#)]
12. Koesling, D.; Mergia, E.; Russwurm, M. Physiological Functions of NO-Sensitive Guanylyl Cyclase Isoforms. *Curr. Med. Chem.* **2016**, *23*, 2653–2665. [[CrossRef](#)] [[PubMed](#)]
13. Gentek, R.; Ghigo, C.; Hoeffel, G.; Bulle, M.J.; Msallam, R.; Gautier, G.; Launay, P.; Chen, J.; Ginhoux, F.; Bajénoff, M. Hemogenic Endothelial Fate Mapping Reveals Dual Developmental Origin of Mast Cells. *Immunity* **2018**, *48*, 1160–1171.e5. [[CrossRef](#)] [[PubMed](#)]
14. St John, A.L.; Rathore, A.P.S.; Ginhoux, F. New perspectives on the origins and heterogeneity of mast cells. *Nat. Rev. Immunol.* **2022**, *23*, 55–68. [[CrossRef](#)]
15. Voehringer, D. Protective and pathological roles of mast cells and basophils. *Nat. Rev. Immunol.* **2013**, *13*, 362–375. [[CrossRef](#)]
16. Palker, T.J.; Dong, G.; Leitner, W.W. Mast cells in innate and adaptive immunity to infection. *Eur. J. Immunol.* **2010**, *40*, 13–18. [[CrossRef](#)]
17. Piliponsky, A.M.; Romani, L. The contribution of mast cells to bacterial and fungal infection immunity. *Immunol. Rev.* **2018**, *282*, 188–197. [[CrossRef](#)]
18. Galli, S.J.; Nakae, S.; Tsai, M. Mast cells in the development of adaptive immune responses. *Nat. Immunol.* **2005**, *6*, 135–142. [[CrossRef](#)]
19. Abraham, S.N.; St John, A.L. Mast cell-orchestrated immunity to pathogens. *Nat. Rev. Immunol.* **2010**, *10*, 440–452. [[CrossRef](#)]
20. Redegeld, F.A.; Yu, Y.; Kumari, S.; Charles, N.; Blank, U. Non-IgE mediated mast cell activation. *Immunol. Rev.* **2018**, *282*, 87–113. [[CrossRef](#)]
21. Galli, S.J.; Tsai, M. IgE and mast cells in allergic disease. *Nat. Med.* **2012**, *18*, 693–704. [[CrossRef](#)] [[PubMed](#)]
22. Mukai, K.; Tsai, M.; Saito, H.; Galli, S.J. Mast cells as sources of cytokines, chemokines, and growth factors. *Immunol. Rev.* **2018**, *282*, 121–150. [[CrossRef](#)] [[PubMed](#)]
23. Lam, H.Y.; Tergaonkar, V.; Kumar, A.P.; Ahn, K.S. Mast cells: Therapeutic targets for COVID-19 and beyond. *IUBMB Life.* **2021**, *73*, 1278–1292. [[CrossRef](#)] [[PubMed](#)]
24. Galli, S.J.; Gaudenzio, N.; Tsai, M. Mast Cells in Inflammation and Disease: Recent Progress and Ongoing Concerns. *Annu. Rev. Immunol.* **2020**, *38*, 49–77. [[CrossRef](#)]
25. Forsythe, P.; Gilchrist, M.; Kulka, M.; Befus, A.D. Mast cells and nitric oxide: Control of production, mechanisms of response. *Int. Immunopharmacol.* **2001**, *1*, 1525–1541. [[CrossRef](#)]
26. Gilchrist, M.; McCauley, S.D.; Befus, A.D. Expression, localization, and regulation of NOS in human mast cell lines: Effects on leukotriene production. *Blood* **2004**, *104*, 462–469. [[CrossRef](#)]
27. Bidri, M.; Féger, F.; Varadaradjalou, S.; Ben Hamouda, N.; Guillosson, J.J.; Arock, M. Mast cells as a source and target for nitric oxide. *Int. Immunopharmacol.* **2001**, *1*, 1543–1558. [[CrossRef](#)]
28. Coleman, J.W. Nitric oxide: A regulator of mast cell activation and mast cell-mediated inflammation. *Clin. Exp. Immunol.* **2002**, *129*, 4–10. [[CrossRef](#)]
29. Davis, B.J.; Flanagan, B.F.; Gilfillan, A.M.; Metcalfe, D.D.; Coleman, J.W. Nitric oxide inhibits IgE-dependent cytokine production and Fos and Jun activation in mast cells. *J. Immunol.* **2004**, *173*, 6914–6920. [[CrossRef](#)]

30. Yip, K.H.; Huang, Y.; Leung, F.P.; Lau, H.Y. Cyclic guanosine monophosphate dependent pathway contributes to human mast cell inhibitory actions of the nitric oxide donor, diethylamine NONOate. *Eur. J. Pharmacol.* **2010**, *632*, 86–92. [[CrossRef](#)]
31. Stasch, J.P.; Schmidt, P.; Alonso-Alija, C.; Apeler, H.; Dembowski, K.; Haerter, M.; Heil, M.; Minuth, T.; Perzborn, E.; Pleiss, U.; et al. NO- and haem-independent activation of soluble guanylyl cyclase: Molecular basis and cardiovascular implications of a new pharmacological principle. *Br. J. Pharmacol.* **2002**, *136*, 773–783. [[CrossRef](#)] [[PubMed](#)]
32. Krieg, T.; Liu, Y.; Rütz, T.; Methner, C.; Yang, X.M.; Dost, T.; Felix, S.B.; Stasch, J.P.; Cohen, M.V.; Downey, J.M. BAY 58-2667, a nitric oxide-independent guanylyl cyclase activator, pharmacologically post-conditions rabbit and rat hearts. *Eur. Heart J.* **2009**, *30*, 1607–1613. [[CrossRef](#)] [[PubMed](#)]
33. Follmann, M.; Griebenow, N.; Hahn, M.G.; Hartung, I.; Mais, F.J.; Mittendorf, J.; Schäfer, M.; Schirok, H.; Stasch, J.P.; Stoll, F.; et al. The chemistry and biology of soluble guanylate cyclase stimulators and activators. *Angew. Chem. Int. Ed. Engl.* **2013**, *52*, 9442–9462. [[CrossRef](#)] [[PubMed](#)]
34. Sandner, P.; Follmann, M.; Becker-Pelster, E.; Hahn, M.G.; Meier, C.; Freitas, C.; Roessig, L.; Stasch, J.P. Soluble GC stimulators and activators: Past, present and future. *Br. J. Pharmacol.* **2021**. [[CrossRef](#)]
35. Jenkinson, H.F. Beyond the oral microbiome. *Environ. Microbiol.* **2011**, *13*, 3077–3087. [[CrossRef](#)]
36. Farges, J.C.; Alliot-Licht, B.; Baudouin, C.; Msika, P.; Bleicher, F.; Carrouel, F. Odontoblast control of dental pulp inflammation triggered by cariogenic bacteria. *Front. Physiol.* **2013**, *4*, 326. [[CrossRef](#)]
37. Kim, D.; Barraza, J.P.; Arthur, R.A.; Hara, A.; Lewis, K.; Liu, Y.; Scisci, E.L.; Hajishengallis, E.; Whiteley, M.; Koo, H. Spatial mapping of polymicrobial communities reveals a precise biogeography associated with human dental caries. *Proc. Natl. Acad. Sci. USA* **2020**, *117*, 12375–12386. [[CrossRef](#)]
38. Galler, K.M.; Weber, M.; Korkmaz, Y.; Widbillier, M.; Feuerer, M. Inflammatory response mechanisms of the dentine-pulp complex and the periapical tissues. *Int. J. Mol. Sci.* **2021**, *22*, 1480. [[CrossRef](#)] [[PubMed](#)]
39. Love, R.M.; Jenkinson, H.F. Invasion of dentinal tubules by oral bacteria. *Crit. Rev. Oral Biol. Med.* **2002**, *13*, 171–183. [[CrossRef](#)]
40. Hahn, C.L.; Liewehr, F.R. Relationships between caries bacteria, host responses, and clinical signs and symptoms of pulpitis. *J. Endod.* **2007**, *33*, 213–219. [[CrossRef](#)]
41. Jontell, M.; Okiji, T.; Dahlgren, U.; Bergenholtz, G. Immune defense mechanisms of the dental pulp. *Crit. Rev. Oral Biol. Med.* **1998**, *9*, 179–200. [[CrossRef](#)] [[PubMed](#)]
42. Goldberg, M.; Farges, J.C.; Lacerda-Pinheiro, S.; Six, N.; Jegat, N.; Decup, F.; Septier, D.; Carrouel, F.; Durand, S.; Chaussain-Miller, C.; et al. Inflammatory and immunological aspects of dental pulp repair. *Pharmacol. Res.* **2008**, *58*, 137–147. [[CrossRef](#)] [[PubMed](#)]
43. Cooper, P.R.; Smith, A.J. Molecular mediators of pulp inflammation and regeneration. *Endod. Top.* **2013**, *28*, 90–105. [[CrossRef](#)]
44. Bischoff, S.C.; Krämer, S. Human mast cells, bacteria, and intestinal immunity. *Immunol. Rev.* **2007**, *217*, 329–337. [[CrossRef](#)] [[PubMed](#)]
45. Chan, C.Y.; St John, A.L.; Abraham, S.N. Plasticity in mast cell responses during bacterial infections. *Curr. Opin. Microbiol.* **2012**, *15*, 78–84. [[CrossRef](#)] [[PubMed](#)]
46. West, P.W.; Bulfone-Paus, S. Mast cell tissue heterogeneity and specificity of immune cell recruitment. *Front. Immunol.* **2022**, *13*, 932090. [[CrossRef](#)] [[PubMed](#)]
47. Zachrisson, B.U. Mast cells in human dental pulp. *Arch. Oral Biol.* **1971**, *16*, 555–556. [[CrossRef](#)]
48. Miller, G.S.; Sternberg, R.N.; Piliro, S.J.; Rosenberg, P.A. Histologic identification of mast cells in human dental pulp. *Oral Surg. Oral Med. Oral Pathol.* **1978**, *46*, 559–566. [[CrossRef](#)]
49. Erdek, Ö.; Bloch, W.; Rink-Notzon, S.; Roggendorf, H.C.; Uzun, S.; Meul, B.; Koch, M.; Neugebauer, J.; Deschner, J.; Korkmaz, Y. Inflammation of the Human Dental Pulp Induces Phosphorylation of eNOS at Thr495 in Blood Vessels. *Biomedicines* **2022**, *10*, 1586. [[CrossRef](#)]
50. Korkmaz, Y.; Lang, H.; Beikler, T.; Cho, B.; Behrends, S.; Bloch, W.; Addicks, K.; Raab, W.H. Irreversible inflammation is associated with decreased levels of the  $\alpha 1$ -,  $\beta 1$ - and  $\alpha 2$ -subunit of sGC in human odontoblasts. *J. Dent. Res.* **2011**, *90*, 517–522. [[CrossRef](#)]
51. Mantovani, A.; Cassatella, M.A.; Costantini, C.; Jaillon, S. Neutrophils in the activation and regulation of innate and adaptive immunity. *Nat. Rev. Immunol.* **2011**, *11*, 519–531. [[CrossRef](#)] [[PubMed](#)]
52. Jaillon, S.; Galdiero, M.R.; Del Prete, D.; Cassatella, M.A.; Garlanda, C.; Mantovani, A. Neutrophils in innate and adaptive immunity. *Semin. Immunopathol.* **2013**, *35*, 377–394. [[CrossRef](#)] [[PubMed](#)]
53. Németh, T.; Sperandio, M.; Mócsai, A. Neutrophils as emerging therapeutic targets. *Nat. Rev. Drug Discov.* **2020**, *19*, 253–275. [[CrossRef](#)] [[PubMed](#)]
54. Rosales, C. Neutrophils at the crossroads of innate and adaptive immunity. *J. Leukoc. Biol.* **2020**, *108*, 377–396. [[CrossRef](#)]
55. Kolaczowska, E.; Kubes, P. Neutrophil recruitment and function in health and inflammation. *Nat. Rev. Immunol.* **2013**, *13*, 159–175. [[CrossRef](#)]
56. De Filippo, K.; Dudeck, A.; Hasenberg, M.; Nye, E.; van Rooijen, N.; Hartmann, K.; Gunzer, M.; Roers, A.; Hogg, N. Mast cell and macrophage chemokines CXCL1/CXCL2 control the early stage of neutrophil recruitment during tissue inflammation. *Blood* **2013**, *121*, 4930–4937. [[CrossRef](#)]
57. Wernersson, S.; Pejler, G. Mast cell secretory granules: Armed for battle. *Nat. Rev. Immunol.* **2014**, *14*, 478–494. [[CrossRef](#)]
58. Dudeck, J.; Kotrba, J.; Immler, R.; Hoffmann, A.; Voss, M.; Alexaki, V.I.; Morton, L.; Jahn, S.R.; Katsoulis-Dimitriou, K.; Winzer, S.; et al. Directional mast cell degranulation of tumor necrosis factor into blood vessels primes neutrophil extravasation. *Immunity* **2021**, *54*, 468–483. [[CrossRef](#)]

59. He, S.; Peng, Q.; Walls, A.F. Potent induction of a neutrophil and eosinophil-rich infiltrate in vivo by human mast cell tryptase: Selective enhancement of eosinophil recruitment by histamine. *J. Immunol.* **1997**, *159*, 6216–6225. [[CrossRef](#)]
60. Huang, C.; Friend, D.S.; Qiu, W.T.; Wong, G.W.; Morales, G.; Hunt, J.; Stevens, R.L. Induction of a selective and persistent extravasation of neutrophils into the peritoneal cavity by tryptase mouse mast cell protease 6. *J. Immunol.* **1998**, *160*, 1910–1919. [[CrossRef](#)]
61. Fullerton, J.N.; Gilroy, D.W. Resolution of inflammation: A new therapeutic frontier. *Nat. Rev. Drug Discov.* **2016**, *15*, 551–567. [[CrossRef](#)] [[PubMed](#)]
62. Kumar, R.; Clermont, G.; Vodovotz, Y.; Chow, C.C. The dynamics of acute inflammation. *J. Theor. Biol.* **2004**, *230*, 145–155. [[CrossRef](#)] [[PubMed](#)]
63. Abudukelimu, A.; Barberis, M.; Redegeld, F.A.; Sahin, N.; Westerhoff, H.V. Predictable Irreversible Switching Between Acute and Chronic Inflammation. *Front. Immunol.* **2018**, *9*, 1596. [[CrossRef](#)] [[PubMed](#)]
64. Lowe, D.B.; Storkus, W.J. Chronic inflammation and immunologic-based constraints in malignant disease. *Immunotherapy* **2011**, *3*, 1265–1274. [[CrossRef](#)]
65. Rodewald, H.R.; Feyerabend, T.B. Widespread immunological functions of mast cells: Fact or fiction? *Immunity* **2012**, *37*, 13–24. [[CrossRef](#)]
66. St John, A.L.; Abraham, S.N. Innate immunity and its regulation by mast cells. *J. Immunol.* **2013**, *190*, 4458–4463. [[CrossRef](#)] [[PubMed](#)]
67. Galli, S.J.; Borregaard, N.; Wynn, T.A. Phenotypic and functional plasticity of cells of innate immunity: Macrophages, mast cells and neutrophils. *Nat. Immunol.* **2011**, *12*, 1035–1044. [[CrossRef](#)]
68. Li, H.; Förstermann, U. Pharmacological prevention of eNOS uncoupling. *Curr. Pharm. Des.* **2014**, *20*, 3595–3606. [[CrossRef](#)] [[PubMed](#)]
69. Karbach, S.; Wenzel, P.; Waisman, A.; Munzel, T.; Daiber, A. eNOS uncoupling in cardiovascular diseases—the role of oxidative stress and inflammation. *Curr. Pharm. Des.* **2014**, *20*, 3579–3594. [[CrossRef](#)]
70. Swindle, E.J.; Metcalfe, D.D. The role of reactive oxygen species and nitric oxide in mast cell-dependent inflammatory processes. *Immunol. Rev.* **2007**, *217*, 186–205. [[CrossRef](#)] [[PubMed](#)]
71. Mittal, M.; Siddiqui, M.R.; Tran, K.; Reddy, S.P.; Malik, A.B. Reactive oxygen species in inflammation and tissue injury. *Antioxid. Redox Signal.* **2014**, *20*, 1126–1167. [[CrossRef](#)] [[PubMed](#)]
72. Di Meo, S.; Reed, T.T.; Venditti, P.; Victor, V.M. Role of ROS and RNS Sources in Physiological and Pathological Conditions. *Oxid. Med. Cell Longev.* **2016**, *2016*, 1245049. [[CrossRef](#)] [[PubMed](#)]
73. Dai, Y.; Faul, E.M.; Ghosh, A.; Stuehr, D.J. NO rapidly mobilizes cellular heme to trigger assembly of its own receptor. *Proc. Natl. Acad. Sci. USA* **2022**, *119*, e2115774119. [[CrossRef](#)] [[PubMed](#)]
74. Korkmaz, Y.; Puladi, B.; Galler, K.; Kämmerer, P.W.; Schröder, A.; Gözl, L.; Sparwasser, T.; Bloch, W.; Friebe, A.; Deschner, J. Inflammation in the Human Periodontium Induces Downregulation of the  $\alpha_1$ - and  $\beta_1$ -Subunits of the sGC in Cementoclasts. *Int. J. Mol. Sci.* **2021**, *22*, 539. [[CrossRef](#)]
75. Korkmaz, Y.; Roggendorf, H.C.; Siefer, O.G.; Seehawer, J.; Imhof, T.; Plomann, M.; Bloch, W.; Friebe, A.; Huebbers, C.U. Downregulation of the  $\alpha_1$ - and  $\beta_1$ -subunit of sGC in Arterial Smooth Muscle Cells of OPSCC Is HPV-Independent. *J. Dent. Res.* **2018**, *97*, 1214–1221. [[CrossRef](#)] [[PubMed](#)]
76. Friebe, A.; Mergia, E.; Dangel, O.; Lange, A.; Koesling, D. Fatal gastrointestinal obstruction and hypertension in mice lacking nitric oxide-sensitive guanylyl cyclase. *Proc. Natl. Acad. Sci. USA* **2007**, *104*, 7699–7704. [[CrossRef](#)]
77. Bankhead, P.; Loughrey, M.B.; Fernández, J.A.; Dombrowski, Y.; McArt, D.G.; Dunne, P.D.; McQuaid, S.; Gray, R.T.; Murray, L.J.; Coleman, H.G.; et al. QuPath: Open source software for digital pathology image analysis. *Sci. Rep.* **2017**, *7*, 16878. [[CrossRef](#)]

**Disclaimer/Publisher’s Note:** The statements, opinions and data contained in all publications are solely those of the individual author(s) and contributor(s) and not of MDPI and/or the editor(s). MDPI and/or the editor(s) disclaim responsibility for any injury to people or property resulting from any ideas, methods, instructions or products referred to in the content.